Lower Branch Coherent States in Shear Flows: Transition and Control

Jue Wang,[1,*] John Gibson,[2,†] and Fabian Waleffe[1,3,‡]

[1]*Department of Mathematics, University of Wisconsin, Madison, Wisconsin 53706, USA*
[2]*Center for Nonlinear Sciences, School of Physics, Georgia Tech, Atlanta, Georgia 30332, USA*
[3]*Department of Engineering Physics, University of Wisconsin, Madison, Wisconsin 53706, USA*

(Received 6 March 2007; published 15 May 2007)

Lower branch coherent states in plane Couette flow have an asymptotic structure that consists of $O(1)$ streaks, $O(R^{-1})$ streamwise rolls and a weak sinusoidal wave that develops a critical layer, for large Reynolds number R. Higher harmonics become negligible. These unstable lower branch states appear to have a single unstable eigenvalue at all Reynolds numbers. These results suggest that lower branch coherent states control transition to turbulence and that they may be promising targets for new turbulence prevention strategies.

DOI: 10.1103/PhysRevLett.98.204501 PACS numbers: 47.27.Cn, 47.27.De, 47.27.ed

Recent experiments indicate that the smallest amplitude necessary to trigger transition to turbulence in pipe flow scales with the inverse of the Reynolds number R, at least for a class of large scale perturbations [1,2]. That R^{-1} scaling, and other characteristics of the perturbations, are shown here to be consistent with a class of unstable 3D traveling wave solutions of the Navier-Stokes equation recently discovered in all canonical shear flows [3–8]. These new *coherent* solutions arise through saddle-node bifurcations at $R = R_{\rm sn}$. At that onset Reynolds number, the solutions capture the form and length scales of the coherent structures that have long been observed in the near wall region of turbulent shear flows [6]. For $R > R_{\rm sn}$, the solutions separate into *upper* and *lower* branches. For relatively low $R > R_{\rm sn}$, a single traveling wave *upper* branch may capture the key statistics of turbulent shear flows remarkably well [6,9,10]. Here it is shown that the *lower* branch solutions in plane Couette flow obey the R^{-1} scaling and evidence is provided that these states form the "backbone" of a phase space boundary separating the basin of attraction of the laminar flow from that of the turbulent flow, and are therefore directly connected with transition to turbulence [5,6,11].

Incompressible fluid flow is governed by the Navier-Stokes equations

$$\partial_t \boldsymbol{v} + \boldsymbol{v}\cdot\boldsymbol{\nabla}\boldsymbol{v} + \boldsymbol{\nabla} p = R^{-1}\nabla^2\boldsymbol{v}, \qquad \boldsymbol{\nabla}\cdot\boldsymbol{v} = 0, \tag{1}$$

where $\boldsymbol{v}(\boldsymbol{r}, t)$ is the fluid velocity at point $\boldsymbol{r}$ and time $t \geq 0$, $p(\boldsymbol{r}, t)$ is the mechanical pressure that enforces incompressibility and $R > 0$ is the Reynolds number which is a nondimensionalized inverse viscosity. The mean flow is in the $\mathbf{e}_x$ direction in a channel with parallel walls at $y = \pm 1$. Plane Couette flow (PCF) is driven by the motion of these walls so $\boldsymbol{v} = \pm\mathbf{e}_x$ at $y = \pm 1$, for all x, z, t, in which case $\boldsymbol{v} = y\mathbf{e}_x$ is the *laminar* solution of (1). That solution is linearly stable for all $R > 0$ [12], but experiments suggest that sustained turbulence exists for $R \gtrsim 325$ [13]. Periodic boundary conditions are imposed in the wall-parallel directions x and z with fundamental wave numbers α and γ, respectively. Further technical information can be found in [6].

For traveling wave solutions, the velocity field is Fourier decomposed in the x direction as

$$\boldsymbol{v}(\boldsymbol{r}, t) = \boldsymbol{v}_0(y, z) + \left(\sum_{n=1}^{\infty} e^{in\theta}\boldsymbol{v}_n(y, z) + \text{c.c.}\right) \tag{2}$$

where $\theta = \alpha(x - ct)$, c is the constant wave velocity and c.c. denotes complex conjugate. The 0-mode $\boldsymbol{v}_0(y, z) = (u_0, v_0, w_0)$ consists of *streamwise rolls* $(0, v_0, w_0)$ with $\partial_y v_0 + \partial_z w_0 = 0$ kinematically decoupled from the streamwise component u_0. The latter consists of an x and z averaged mean flow $\bar{u}(y)$ and *streaks* $u_0(y, z) - \bar{u}(y)$.

Symmetric lower branch traveling waves in plane Couette flow (for which $c = 0$) have been continued to high R by Newton's method as in [3,4,6]. Figure 1 shows the scaling of the amplitudes of the various elements constituting such solutions as functions of R. The streaks $u_0(y, z) - \bar{u}(y)$ tend to a nonzero constant while the amplitude of the rolls $(0, v_0(y, z), w_0(y, z))$ scales like R^{-1} as $R \to \infty$. The fundamental mode $\boldsymbol{v}_1(y, z)$ has an approximate $R^{-0.9}$ scaling, while the 2nd and 3rd harmonics scale approximately like $R^{-1.6}$ and $R^{-2.2}$, respectively. Higher harmonics decay faster and are not shown. This separation between the harmonics suggests that the 2nd and higher harmonics become insignificant for large R. Indeed, the solution was continued beyond $R = 6168$ by dropping all harmonics with no significant change. This asymptotic structure confirms, and is understood by, the asymptotic form of the *self-sustaining process* [11,14]. That process consists of R^{-1} streamwise rolls $(0, v_0, w_0)$ redistributing the streamwise velocity u to create $O(1)$ streaks $u_0(y, z) - \bar{u}(y)$ whose inflectional instability leads to an $e^{i\theta}\boldsymbol{v}_1(y, z)$ wave whose nonlinear self-interaction feeds back on the streamwise rolls, leading to the existence of invariant states and departure from the laminar flow. That mechanistic theory is directly tied to the methods used to compute coherent states in all canonical shear flows [3,4,6–8].

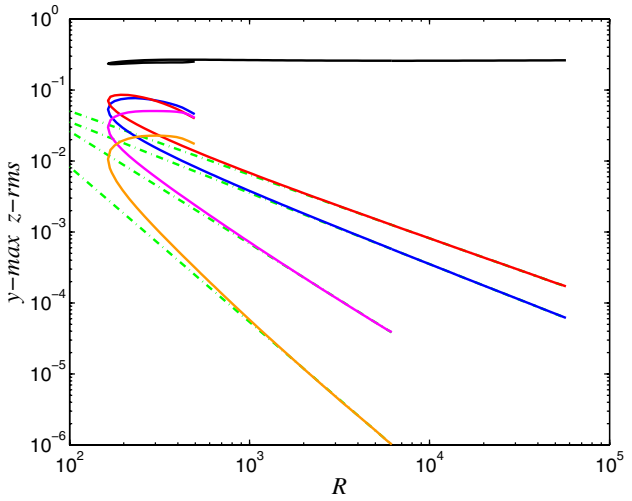

FIG. 1 (color online). Amplitude of x-Fourier modes for a 3D steady state in plane Couette flow vs R for $(\alpha, \gamma) = (1, 2)$. Top to bottom: $O(1)$ streak $u_0(y, z) - \bar{u}(y)$, $O(R^{-0.9})$ fundamental mode $|w_1|$, $O(R^{-1})$ streamwise rolls (v_0, w_0) and $o(R^{-1})$ $|\boldsymbol{v}_2|$ and $|\boldsymbol{v}_3|$. Continued beyond $R = 6168$ by dropping all harmonics. $R_{\rm sn} \approx 164$ is the turning point where lower and upper branch solutions coalesce.

Figure 2 illustrates the structure of the lower branch steady state. The streaky flow $u_0(y, z)$ and the rolls $(0, v_0, w_0)$ remain large scale and their structure becomes independent of R; v_0 has a simple updraft at $z = 0$ and downdraft at $z = \pm\pi/\gamma$ that sustain the z modulation of $u_0(y, z)$ (recall that $u_0 = \pm 1$ at $y = \pm 1$ in PCF). But the fundamental mode $\boldsymbol{v}_1$ concentrates about the *critical layer* $u_0(y, z) = c$ ($c = 0$ for these states in PCF). Critical layers are well known in the context of the 2D, linear theory of shear flows [15]. Here the critical layer is a surface in 3D space and it is nonlinearly coupled to the 0-mode $\boldsymbol{v}_0(y, z)$. When the higher harmonics become negligible and $|v_0|$, $|w_0| \ll |u_0|$, the equation for the fundamental mode simplifies to [11,14,16]

$$[i\alpha(u_0 - c)\boldsymbol{v}_1 + (\boldsymbol{v}_1 \cdot \boldsymbol{\nabla} u_0)\mathbf{e}_x]e^{i\theta} = -\nabla(p_1 e^{i\theta}) + R^{-1}\nabla^2(\boldsymbol{v}_1 e^{i\theta}), \quad (3)$$

with $\boldsymbol{\nabla} \cdot (\boldsymbol{v}_1 e^{i\theta}) = 0$. For high R, the solutions develop an $R^{-1/3}$ critical layer in the neighborhood of $u_0(y, z) - c = 0$ that results from the balance between $\alpha(u_0 - c) = \alpha(\boldsymbol{r} - \boldsymbol{r}_c) \cdot \boldsymbol{\nabla} u_0 + O(|\boldsymbol{r} - \boldsymbol{r}_c|^2)$ and $R^{-1}\nabla^2$, so if δ is the critical layer thickness, we must have $\alpha\delta|\boldsymbol{\nabla} u_0| \sim R^{-1}\delta^{-2}$ and $\delta \sim (\alpha|\boldsymbol{\nabla} u_0|R)^{-1/3}$ near $u_0(y, z) - c = 0$. Figure 3 confirms that critical layer scaling for the lower branch steady state in PCF.

The nonlinear coupling between the fundamental $\boldsymbol{v}_1$, with its critical layer structure, and the rolls (v_0, w_0) provides a challenge for the development of a full asymptotic theory of the lower branch states that would be able to predict the amplitude scaling of the fundamental mode. If $\boldsymbol{v}_1$ remained a large scale structure, its amplitude would have to scale like R^{-1} in order for its nonlinear self-

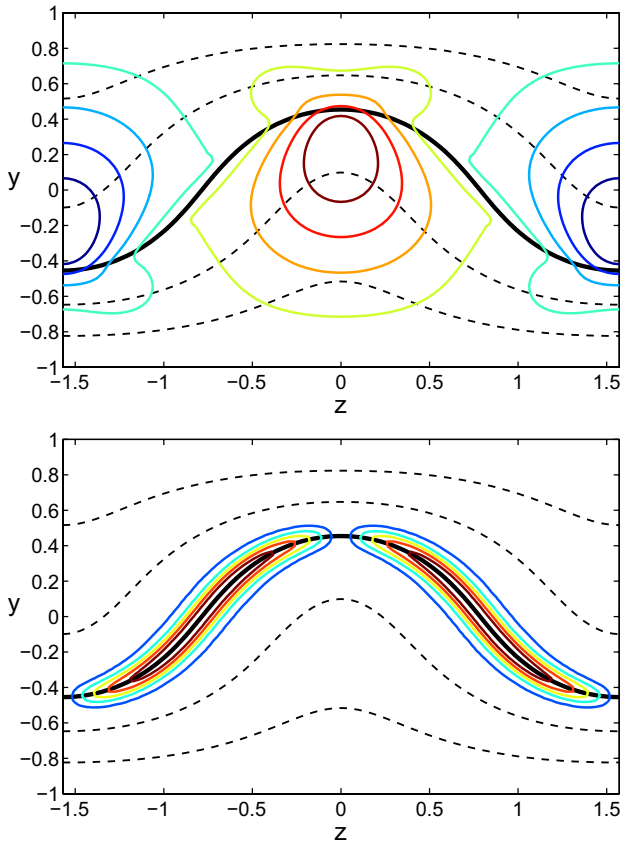

FIG. 2 (color online). Contours of $v_0(y, z)$ (solid, top) and $|v_1(y, z)|$ (solid, bottom) both with contours of $u_0(y, z) = [-2{:}2]/3$ (dashed) for $(\alpha, \gamma, R) = (1, 2, 50\,171)$. The critical layer $u_0(y, z) = 0$ is shown as a bold solid curve in both plots. Top (bottom) wall at $y = 1$ (-1) moves into (out of) the page so no-slip boundary conditions impose $u_0(\pm 1, z) = \pm 1$ and $v_0(\pm 1, z) = 0$.

interaction to balance the viscous diffusion of the R^{-1} streamwise rolls v_0 [11,14]. The development of a critical layer scale complicates the analysis and different norms and components have different scalings. Nonetheless, an

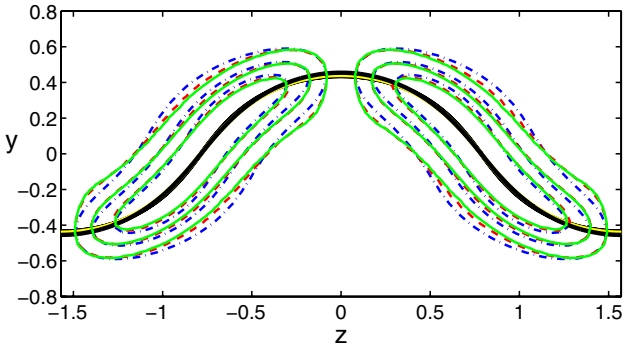

FIG. 3 (color online). Contours of $|v_1|$ for $(\alpha, \gamma) = (1, 2)$ at $R = 50\,171$ (solid) and 12 637 (dashed) stretched by $R^{1/3}$ factors along curves normal to u_0 contours to match $|v_1|$ contours at $R = 3079$ (dash-dot line). The (almost overlapping) black and yellow solid curves show $u_0(y, z) = 0$ at the 3 R's.

asymptotic theory appears feasible and the present numerical data is clear and its implications are significant: the lower branch states tend to a relatively simple but nontrivial quasi-2D singular asymptotic state as $R \to \infty$ that is *not* a solution of the Euler equation [Eq. (1) with $R^{-1} = 0$], and that is *not* the laminar flow $\boldsymbol{v} = y\mathbf{e}_x$ either. So the lower branch states do not bifurcate from the laminar flow, not even at $R = \infty$. The data presented is for $(\alpha, \gamma) = (1, 2)$, however, identical features hold for other (α, γ) values.

Turning now to a stability analysis of the lower branch coherent states we find that these states are distinguished not only by their asymptotic structure but also by their stability characteristics. Our eigenmode analysis of the 3D lower branch steady state in plane Couette flow, up to $R = 12\,000$, show that they have a *single*, real unstable eigenvalue shown in Fig. 4 for $(\alpha, \gamma) = (1.14, 2.5)$. This state is most unstable at $R \approx 342$ then the unstable eigenvalue steadily decreases approximately as $R^{-0.48}$ for larger R. Furthermore, the corresponding eigenfunction is in the same shift-reflect and shift-rotate symmetries [[6], Eqs. (24), (26)] as the lower branch state. This is not true for the upper branch states which develop new bifurcations and unstable modes as R increases.

These stability results were obtained using both a direct calculation of the eigenvalues of the full Jacobian in the doubly symmetric subspace of the lower branch state with an ellipsoidal truncation of the Fourier-Chebyshev representation [6], and an iterative calculation in the full space using the Arnoldi algorithm and the CHANNELFLOW code with cubic truncation [17]. The leading unstable and least stable eigenvalues matched to 5 or 6 significant digits. We have also investigated subharmonic instabilities through numerical simulations in a double-sized box with fundamental wavenumbers $\alpha/2$ and $\gamma/2$. For $R = 1000$ and $(\alpha, \gamma) = (1.14, 2.5)$, the fundamental instability shown in Fig. 4 has growth rate 0.036 81, we also found a weak instability subharmonic in x with growth rate $0.005\,248 \pm i0.022\,45$. The analysis of this subharmonic mode is left for future study.

Thus, in the one-period domain with fundamental wave numbers (α, γ), the lower branch state is an unstable equilibrium with a 1D unstable manifold. Therefore its stable manifold splits the phase space into two parts, at least locally. The evolution of disturbances in the one-period domain, starting on the 1D unstable manifold of the lower branch on either side of the stable manifold is illustrated in Fig. 5. These numerical simulations were performed using CHANNELFLOW in the full phase space and show the time evolutions in the energy input-energy dissipation plane, both normalized by their laminar values. For plane Couette flow, the normalized energy input rate is equal to the normalized drag, that is, the drag at the walls normalized by their laminar value. Perturbations starting on one side of the stable manifold gently decay back to the linearly stable laminar flow $\boldsymbol{v} = y\mathbf{e}_x$ while perturbations on the other side of the stable manifold shoot to a turbulent state. Figure 5 also shows the upper branch brother of the lower branch state which, as stated earlier, is located in phase space much closer to the "turbulent" state. The decay of perturbed lower branch states back to the laminar flow follows a standard two-step evolution. First, the fundamental mode $\boldsymbol{v}_1$, with its critical layer structure, disappears and the flow relaxes to an x-independent state that consists of streamwise rolls $(0, v_0, w_0)$ and streaks $u_0(y, z)$ and slowly decays back to the laminar flow on a long viscous time scale. Perturbations that shoot to a turbulent state follow a much more rapid "breakdown" (as indicated by the $\Delta t = 5$ dot spacing in Fig. 5) with high dissipation rate (about 13 on Fig. 5) then settle to a turbulent state with energy input and dissipation rates of about 4.4 [for $(\alpha, \gamma, R) = (1, 2, 1000)$].

These results show that the lower branch stable manifold is a piece of the boundary separating the basin of attraction of the laminar state from that of the turbulent state. Our results have focused on symmetric steady states in plane Couette flow but there is evidence of a similar role for lower branch traveling waves in plane Poiseuille flow [5] and pipe flow [18]. Recent work by Viswanath [19] complements our work by showing that perturbations of the

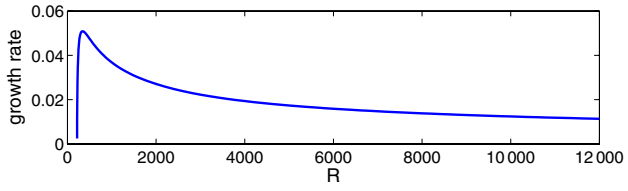

FIG. 4 (color online). The single unstable eigenvalue of the lower branch state $(\alpha, \gamma) = (1.14, 2.5)$ as function of R. Asympotic scaling is $\approx O(R^{-0.48})$. There is an extra complex conjugate pair near the onset $R_{sn} \approx 218$.

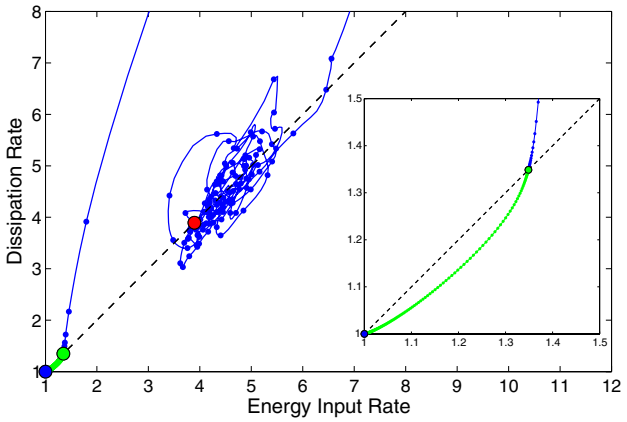

FIG. 5 (color online). Energy input/dissipation rate starting near the lower branch fixed point $(\alpha, \gamma, R) = (1, 2, 1000)$ on its unstable manifold. In one direction, the flow goes to turbulence while in the other direction it relaminarizes. The dot spacing is $\triangle t = 5$. The blue marker at (1,1) is the laminar flow, green marker at (1.35,1.35) is the lower branch state and the red marker at (3.89,3.89) is its upper branch brother.

laminar flow in the form of streamwise rolls of the right threshold amplitude + small 3D noise do get attracted to a lower branch state before shooting to turbulence. We expect the symmetric lower branch state to play a key role for transition in plane Couette flow but there exist other asymmetric lower branch traveling wave states as well as periodic orbits [19–21], each of which may play a similar ''transition-backbone'' role, locally in phase space. We conjecture that the invariant states (steady states, traveling waves, and periodic orbits) most relevant to transition to turbulence will contain R^{-1} streamwise rolls. It may be possible to trigger transition with smaller disturbances but we suspect that such disturbances would lead to the formation of an R^{-1} updraft (as in Fig. 2, top) which in turn would create $O(1)$ streaks and an approach toward a lower branch state with R^{-1} rolls and $O(1)$ streaks thanks to the sustenance of the rolls from the nonlinear interaction of the streak wave $e^{i\theta}\boldsymbol{v}_1(y,z)$, prior to transition along the unstable manifold of the lower branch state. This scenario is consistent with the experiments [1] where transition is triggered by a jet from the wall of amplitude R^{-1} and of sufficient duration, as well as with the simulations in [19].

The extreme low dimensionality of the lower branch unstable manifold suggests a new approach to turbulence control. Turbulence control strategies roughly fall into 2 categories: either prevent nonlinear breakdown of the linearly stable laminar flow, or push the fully nonlinear turbulent flow back to laminar. A new strategy might be to put the flow on a lower branch equilibria and keep it there by controlling its very few unstable modes. There would be a small drag penalty to do so since lower branch states have a net drag that is 30% to 40% higher than the *laminar* state as $R \rightarrow \infty$ but that would still correspond to a near 100% drag reduction, as $R \rightarrow \infty$, when compared to the turbulent state. This control strategy is related to, but quite distinct from the strategies proposed in [22,23]. Streaks are used in [23] to efficiently deform the laminar base flow in order to prevent the *linear* instability of boundary layer flow. In [22] strategies are considered to push the turbulent flow onto the laminar side of the stable manifold of a lower branch unstable periodic solution in order to relaminarize the flow. The current proposal is to put the flow on the unstable lower branch equilibrium and keep it there by controlling its few unstable eigenmodes.

The data discussed in this Letter as well as movies illustrating the return to laminar and the turbulent breakdown displayed in Fig. 5 are posted at [24].

J. W. and F. W. were partially supported by NSF Grant No. DMS-0204636. We thank Divakar Viswanath and Predrag Cvitanović for helpful discussions.

*Electronic address: wang@math.wisc.edu
†Electronic address: gibson@cns.physics.gatech.edu
‡Electronic address: waleffe@math.wisc.edu

[1] B. Hof, A. Juel, and T. Mullin, Phys. Rev. Lett. **91**, 244502 (2003).
[2] R. Fitzgerald, Phys. Today **57**, No. 2, 21 (2004).
[3] F. Waleffe, Phys. Rev. Lett. **81**, 4140 (1998).
[4] F. Waleffe, J. Fluid Mech. **435**, 93 (2001).
[5] T. Itano and S. Toh, J. Phys. Soc. Jpn. **70**, 703 (2001).
[6] F. Waleffe, Phys. Fluids **15**, 1517 (2003).
[7] H. Faisst and B. Eckhardt, Phys. Rev. Lett. **91**, 224502 (2003).
[8] H. Wedin and R. Kerswell, J. Fluid Mech. **508**, 333 (2004).
[9] J. Jimenez, G. Kawahara, M. Simens, and M. Nagata, Phys. Fluids **17**, 015105 (2005).
[10] B. Hof, C. van Doorne, J. Westerweel, F. Nieuwstadt, H. Faisst, B. Eckhardt, H. Wedin, R. Kerswell, and F. Waleffe, Science **305**, 1594 (2004).
[11] F. Waleffe, Phys. Fluids **9**, 883 (1997).
[12] V. Romanov, Funct. Anal. Appl. **7**, 137 (1973).
[13] S. Bottin, O. Dauchot, and F. Daviaud, Phys. Rev. Lett. **79**, 4377 (1997).
[14] F. Waleffe, Stud. Appl. Math. **95**, 319 (1995).
[15] S. Maslowe, Annu. Rev. Fluid Mech. **18**, 405 (1986).
[16] D. Benney, Stud. Appl. Math. **70**, 1 (1984).
[17] J. F. Gibson, http://www.channelflow.org.
[18] R. Kerswell and O. Tutty, arXiv:physics/0611009 [J. Fluid Mech. (to be published)].
[19] D. Viswanath, arXiv:physics/0701337.
[20] D. Viswanath, J. Fluid Mech. **580**, 339 (2007).
[21] G. Kawahara and S. Kida, J. Fluid Mech. **449**, 291 (2001).
[22] G. Kawahara, Phys. Fluids **17**, 041702 (2005).
[23] J. Fransson, A. Talamelli, L. Brandt, and C. Cossu, Phys. Rev. Lett. **96**, 064501 (2006).
[24] http://www.math.wisc.edu/~waleffe/ECS/.